

# Passive Damping of the Forced Precession Motion of a Two-Body Satellite

WAI K. LIM\*

*Jet Propulsion Laboratory, Pasadena, Calif.*

The two-body satellite under study consists of two axisymmetric rigid bodies interconnected by a lossy universal joint that ensures a common axial spin but dissipates energy when there is lateral relative motion. The external torque acting on the system is assumed to be perpendicular to the symmetry axis of one body and an external fixed direction. This paper is concerned with the analysis and analytical design of this system for fast damping of its transient oscillations. Two methods have been developed for the computation of the decay time  $t_D$  of the forced precession cone angle; one is based on energy consideration and the other on angular momentum consideration. The dependences of  $t_D$  on each of the physical parameters of the system were investigated. For an especially simple near-optimum configuration, an analytic solution for  $t_D$  was obtained. The newly developed theory was applied in an example to the design of a small sun-pointing interplanetary probe oriented by a solar sail.

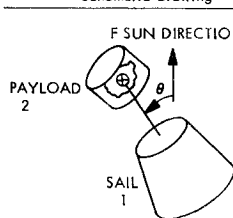
## Nomenclature

$a$	$= \sin \theta_0 / \alpha_m$
$A, B, C$	$=$ principal moments of inertia of $P$
$A'$	$=$ transverse moments of inertia of body $P$ about the joint
$A', B'$	$= A + dm_s m_p / (m_s + m_p), B + dm_s m_p / (m_s + m_p)$
$c, k$	$=$ respectively, the viscous coefficient and spring constant of each degree of freedom of the universal joint
$C_{\alpha}, S_{\alpha}$	$= \cos \alpha, \sin \alpha$
$d$	$=$ distance from the center of mass of $P$ to the joint
$D, K$	$= c/I_1, k/I_1$
$I_1, I_2, I_3$	$=$ principal moments of inertia of $S$
$\mathbf{M}$	$=$ the resultant internal torque at the joint acting on $S$
$p, q, r$	$=$ the absolute angular velocity of body $P$ projected on the $\hat{X}_p, \hat{Y}_p, \hat{Z}_p$ axis
$P$	$=$ external precession torque constant (precession torque $= P \sin \theta$ )
$r_0$	$=$ initial spin rate of bodies 1 and 2
$t(\theta)$	$=$ decay time of the precession cone angle from $\theta_0$ to $\theta$
$\mathbf{T}_p$	$=$ the external torque acting on $P$ about its center of mass
$W_1, W_2, W_3$	$=$ the absolute angular velocity of $S$ projected on its principal axis
$\hat{X}_p, \hat{Y}_p, \hat{Z}_p$	$=$ unit vectors along a set of body-fixed principal axes of body $P$ with its origin at the center of mass of $P$
$\hat{X}_s, \hat{Y}_s, \hat{Z}_s$	$=$ unit vectors along a set of body-fixed principal axes of body $S$ with its origin at the center of mass of $S$
$\alpha, \beta$	$=$ relative rotations of body $S$ with respect to body $P$ in the directions of $\hat{X}_p$ and $\hat{Y}_s$ , respectively
$\alpha_m$	$=$ maximum allowable deflection between bodies 1 and 2
$\theta$	$=$ forced precession cone angle; $\theta_0 =$ initial $\theta$
$\theta_1, \theta_2, \theta_3$	$=$ Euler angles which define the orientation of the $\hat{X}_p, \hat{Y}_p, \hat{Z}_p$ axes (see Fig. 1) with respect to an external reference coordinate
$\rho, \sigma_1, \sigma_2$	$= I_1/A', C/A',$ and $I_3/I_1$ , respectively
$\omega_L$	$= (P/A')^{1/2}$

## Introduction

DONATONI<sup>1</sup> proposed a new concept of passive attitude control of an interplanetary spacecraft that aligns the spin axis of the vehicle with the sun. The system consists of a payload and a conical solar sail connected by a lossy universal joint, which ensures a common spin but that dissipates energy when there is lateral relative motion (see Table 1). At injection, the spin axis of the system is at a large angle (say,  $60^\circ$ ) away from the sun. Without the universal joint, solar-pressure-torque acting on the system will precess the spin axis about the sun-line at a cone angle  $\theta$  equal to this initial misalignment. Damping introduced by the relative motion between the two bodies causes the decay of the  $\theta$ . Because of the extremely slow precession rate of the system derived from the solar-radiation torque (precession period is of the order of days), fast damping of  $\theta$  is crucial to the usefulness of this attitude orientation scheme. This paper presents a simplified theory for the decay of  $\theta$  and some general results related to the design of this two-body system for fast damping.

Table 1 Two-body system

Forced Precession Damper		
Schematic Drawing	Description	
	TWO SPINNING AXISYMMETRIC RIGID BODIES CONNECTED BY A LOSSY UNIVERSAL JOINT LOCATED AT THE CENTER OF MASS OF BODY 2.	
Damper design		
$K/r_0^2$	$D/r_0$	$t(\theta)$
0	$\alpha \left( \frac{\omega_L}{r_0} \right)^2 \left( \frac{1}{1+\rho} \right)$	$\frac{t(\theta)}{T_D} = \sin \theta_0 \cos^2 \theta_0 \left[ \left( \frac{1}{\cos^2 \theta_0} - \frac{1}{\cos^2 \theta} \right) + 2 \ln \left( \frac{\tan \theta_0}{\tan \theta} \right) \right]$ $T_D = \frac{1}{2} \left( \frac{r_0}{\omega_L} \right) \frac{(1+\rho)^2}{\rho} \frac{1}{\alpha_m}$

Received February 24, 1970; revision received August 3, 1970. This paper presents the results of one phase of research carried out at the Jet Propulsion Laboratory, California Institute of Technology, under Contract NAS 7-100, sponsored by NASA. The research was part of the author's doctoral dissertation.

\* Resident Research Associate; formerly Research Assistant, MIT Measurement Systems Laboratory, Cambridge, Mass. Member AIAA.

Methods of orientation by solar-radiation pressure suitable for nonspinning vehicles have been described by Sohn,<sup>2</sup> Frye and Sterns,<sup>3</sup> Hibbard,<sup>4</sup> Acord and Nicklas,<sup>5</sup> and many others. Sohn proposed the use of a weathervane-type system; Frye and Stearns suggested that a trailing cone be used; Hibbard proposed that focused radiation could be used as a powerful restoring force by flanking the collector surface with a reflector. Acord and Nicklas analyzed and designed an articulated solar vane as a primary attitude control system. Methods that are intended for spinning vehicles have been described by Ule,<sup>6</sup> Peterson,<sup>7</sup> Columbo,<sup>8</sup> and Falcovitz.<sup>9</sup> Ule's scheme uses a corner mirror array fixed to the vehicle which produces a second-order despin torque in addition to the precession torque. Peterson studied the possibility of using the thermal reradiation effect of a solar sail. Columbo analyzed the general behavior of a spinning satellite subjected to orthogonal-erecting torque and proposed to maintain the spin rate by using a radial solar vane. Falcovitz investigated the design and application of optically asymmetric sails, which produce both an erecting torque and the precession torque.

The present method differs from previous methods in that it involves the dynamics of two flexibly interconnected rigid bodies instead of one. The present system differs from that of Donatoni<sup>1</sup> in one respect; that is, the universal joint is located at the center of mass of the payload rather than of the sail.

### Basic Forced Precessional Motion

Lack of space makes it necessary to omit derivation of the exact equations of motion of the system, but the equations are presented in the Appendix. However, to provide a basis for the discussion on the dynamics of this two-body system, we will briefly review the basic forced precessional motion of a single spinning axisymmetric rigid body. In Fig. 1, the external torque  $T_p$  acting on the rigid body is assumed to be perpendicular to both the symmetry axis  $z$  and the external reference axis  $\hat{u}_s$ , which coincides with  $Z$ :

$$T_p = -[P(\hat{u}_s \times \hat{z})]/|\hat{u}_s \times \hat{z}| \quad (1)$$

where  $P$  is a torque constant. The kinematic relationships between the Euler angles and the components of angular velocity of the body  $p, q, r$  are as follows:

$$\dot{\theta}_1 = (-p \cos \theta_3 + q \sin \theta_3)/\sin \theta_2 \quad (2a)$$

$$\dot{\theta}_2 = p \sin \theta_3 + q \cos \theta_3 \quad (2b)$$

$$\dot{\theta}_3 = r + \cot \theta_2(p \cos \theta_3 - q \sin \theta_3) \quad (2c)$$

In terms of  $p, q$ , and  $r$ , the Euler equations of motion of the system reduce to

$$\dot{p} = -(\sigma - 1)qr + (T_{px})/A \quad (3a)$$

$$\dot{q} = (\sigma - 1)pr + (T_{py})/A, \quad \dot{r} = (T_{pz})/C \quad (3b)$$

where  $\sigma = C/A$ ;  $C$  and  $A$  are, respectively, the axial and

transverse moment of inertia of the body. The projections of  $T_p$  onto the principal coordinates  $x, y, z$  can be shown to be:

$$\begin{bmatrix} T_{px} \\ T_{py} \\ T_{pz} \end{bmatrix} = -P \sin \theta_2 \begin{bmatrix} \sin \theta_3 \\ \cos \theta_3 \\ 0 \end{bmatrix} \quad (4)$$

When the external torque is small, such that the forced precession rate of the spin axis  $z$  is slow compared with the nutation frequency  $\sigma r$ , one can substitute  $\theta$ , the average value of  $\theta_2$  over one nutation cycle, into Eqs. (3) and (4). The solutions of  $p$  and  $q$  are then obtained as follows:

$$p = -\Omega [\cos(\sigma - 1)rt - \cos rt] \quad (5a)$$

$$q = -\Omega [\sin(\sigma - 1)rt + \sin rt] \quad (5b)$$

$$r = \text{constant} \quad (5c)$$

where  $\Omega = P \sin \theta / Cr$ .

The initial conditions on  $p$  and  $q$  have been assumed to be both zero in deriving Eq. (5). Substitution of Eq. (5) into Eq. (2) leads to the time history of the Euler angles:

$$\theta_1 = -\Omega[t - (1/\sigma r) \sin \sigma r t] \quad (6a)$$

$$\theta_2 = \theta + (\Omega/\sigma r) \cos \sigma r t \quad (6b)$$

Equation (6) shows the forced precession and nutation motions of a fast spinning top;  $\Omega$  and  $\sigma r$  can be identified as the precession and nutation frequency, respectively;  $\theta$  is the mean precession cone angle.

### Energy Approach

Now replace mentally the single rigid body in the previous section by the two-body system shown in Table 1. Since the surface area of the payload is much smaller than the sail, it is assumed that solar-pressure-torque acts only on the sail. An important characteristic of the forced precession motion of this system is that since the external torque is perpendicular to the fixed reference direction  $\hat{u}_s$ , the component of the total angular momentum  $\mathbf{H}$  along  $\hat{u}_s$  is a constant of motion, i.e.,

$$H_z = \mathbf{H} \times \hat{u}_s \quad (7)$$

The analysis is based on the following two assumptions: a) the potential energy of the system associated with the solar-radiation torque is small compared with its spin kinetic energy, and b) the nutation angle of the sail is small. Under these assumptions, the angular momentum vector  $\mathbf{H}$  approximately coincides with the spin axis  $\hat{z}$  and we can write the following equations:

$$H_z \cong H \cos \theta, H \cong Cr + I_3 W_3 \quad (8)$$

$$E \cong \frac{1}{2}(Cr^2 + I_3 W_3^2) \quad (9)$$

where  $C$  and  $I_3$  are, respectively, the axial moments of inertia of the sail and payload;  $r$  and  $W_3$  are their respective inertial angular velocities. Because of the nature of the universal joint connecting them, the two parts of the system must have the same average spin rate. (Their instantaneous values may be different however, because  $r$  and  $W_3$  are referred to their respective body frames whose relative motion has so far been neglected.) We can then obtain

$$\dot{H}/H = \dot{E}/2E \quad (10)$$

Differentiation of Eq. (8) and substitution into Eq. (10) leads to

$$d/dt(\ln \cos \theta) = -\frac{1}{2}\dot{E}/E \quad (11)$$

In other words, the decay rate of  $\ln \cos \theta$  is proportional to the relative rate of energy dissipation of the system. If  $\dot{E}/E$  can be computed as a function of  $\theta$ , the damping time of

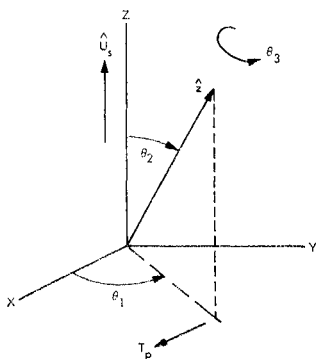


Fig. 1 Kinematics of forced precession.

$\theta$  is obtainable by integrating Eq. (11):

$$t(\theta_f, \theta_0) = 2 \int_{\cos \theta_0}^{\cos \theta_f} \frac{d(\ln \cos \theta)}{(-\dot{E}/E)} \quad (12)$$

### Despin Torque Approach

From Eq. (8), it is seen that if  $\theta$  is to be reduced to zero from an initially large angle, the magnitude of  $\mathbf{H}$  must decrease. Based on this argument, a different approach to the precession damping problem is to first compute  $t_r$ , the time it takes for the system to despin. Since  $\theta$  can be related to the spin rate through Eq. (8),  $t(\theta_f, \theta_0)$  can be inferred from  $t_r$ .

From the Appendix we have the exact equations [Eqs. (A1, A2, and A5)] of the spin rate  $r$  and  $W_3$  of the sail and the payload, respectively, which, with axial symmetry and with the component of solar torque along the sail axis assumed zero, become

$$C\dot{r} = -M_\beta \sin \alpha - M_z \cos \alpha \quad (13)$$

$$I_3 \dot{W}_3 = M_\alpha \sin \beta + M_z \cos \beta \quad (14)$$

$c$  and  $k$  are, respectively, the viscous coefficient and the spring constant of the joint;  $\alpha$  and  $\beta$  are the two successive rotations of the payload with respect to the sail. Eliminate  $M_z$  from the two equations above:

$$(C\dot{r}/\cos \alpha) + (I_3 \dot{W}_3/\cos \beta) = -M_\beta \tan \alpha + M_\alpha \tan \beta \quad (15)$$

We will evaluate the RHS of Eq. (15) by assuming a quasi-steady deflection angle of the sail with respect to the payload. This appears as oscillations in  $\alpha$  and  $\beta$  at the spin rate  $r$ :

$$\alpha = A_\alpha \sin(rt + \Psi), \beta = A_\beta \cos(rt + \Psi) \quad (16)$$

where  $A_\alpha$  and  $A_\beta$  are defined as the unknown amplitudes of oscillation of  $\alpha$  and  $\beta$ , respectively;  $\Psi$  is the unknown phase angle of  $\alpha$  with respect to the external torque  $T_{pz}$ . Because of the symmetry in  $\alpha$  and  $\beta$ , it is expected that  $A_\alpha$  equals  $A_\beta$ . Substitute Eq. (16) into Eq. (15) and average over one spin period,  $2\pi/r$ . The spring terms drop out and the damping terms give a net average retarding torque as

$$C \left\langle \frac{\dot{r}}{\cos \alpha} \right\rangle + I_3 \left\langle \frac{\dot{W}_3}{\cos \beta} \right\rangle = -\frac{g}{2} cr(A_\alpha^2 + A_\beta^2) \quad (17)$$

where  $g$  is an amplitude correction factor which is defined by

$$g = \frac{2}{A_\alpha} \int_0^{2\pi} d\xi \cos \xi \tan(A_\alpha \cos \xi) \quad (18)$$

When  $A_\alpha$  and  $A_\beta$  become small angles,  $g$  approaches 1.

The interpretation of the LHS of Eq. (17) is as follows. Because of the nature of the universal joint, the two bodies must, in the average, despin at the same rate and  $\langle \dot{r}/\cos \alpha \rangle$  equals  $\langle \dot{W}_3/\cos \beta \rangle$ . Therefore,

$$\langle \dot{r} \rangle = -cr(A_\alpha^2 + A_\beta^2)g/2(C + I_3) \quad (19)$$

Equation (19) is the average despin rate of the system. It can be integrated to give the decay time of the spin rate  $r$ .

$$t_r(r_f, r_0) = 2 \left[ \frac{(C + I_3)}{gc} \right] \int_{r_0}^{r_f} \frac{dr}{r(A_\alpha^2 + A_\beta^2)} \quad (20)$$

### Design of a Forced Precession Damping System

In the last two sections, we showed the procedures for computing the decay time of the forced precession cone angle  $\theta$  once the damper amplitudes  $A_\alpha$  and  $A_\beta$  are known. In general  $A_\alpha$  and  $A_\beta$  are difficult to obtain except by numerical integration. However, if in addition to the basic assumptions of slow precession and small nutation angle, we assume that  $\alpha$  and  $\beta$  are small angles, then the problem can be linearized. In this section we will compute  $A_\alpha, A_\beta$  from

the linearized equations of motion of the system and discuss the problems of configuration selection and parameters optimization for fast damping of  $\theta$ . For a system of such complexity, linear analysis results provide qualitatively useful information.

Assuming that  $r$  and  $W_3$  predominate (all other state variables  $p, q, \alpha, \beta, \dot{\alpha}, \dot{\beta}$  being small), the following linear systems can be obtained from Eqs. (A1) and (A2):

$$\dot{p} - (1 - \sigma_1)qr - \rho(K\alpha + D\dot{\alpha}) = -\left(\frac{P}{A'}\right) \sin \theta \sin rt \quad (21a)$$

$$\dot{q} + (1 - \sigma_1)pr - \rho(K\beta + D\dot{\beta}) = -\left(\frac{P}{A'}\right) \sin \theta \cos rt \quad (21b)$$

$$\ddot{\alpha} + D\dot{\alpha} + K\alpha + (\sigma_2 - 1)r^2\alpha + (\sigma_2 - 2)r\dot{\beta} = -\dot{p} + (1 - \sigma_2)qr \quad (22a)$$

$$\ddot{\beta} + D\dot{\beta} + K\beta + (\sigma_2 - 1)r^2\beta - (\sigma_2 - 2)r\dot{\alpha} = -\dot{q} - (1 - \sigma_2)pr \quad (22b)$$

where  $\sigma_1 = C/A'$ ,  $\sigma_2 = I_3/I_1$ ,  $\rho = I_1/A'$ ,  $K = k/I_1$ , and  $D = c/I_1$ .

One can think of the RHS of Eq. (21) as the forcing function to this sixth-order system. Its amplitude is proportional to the external torque  $P \sin \theta$  and its frequency is the instantaneous spin rate  $r$ . The following five parameters are pertinent in the design of this system: a)  $\rho$ , the ratio between the moment of inertia of the payload to that of the sail; b)  $\sigma_1$  and  $\sigma_2$ , the ratios between the axial and transverse moments of inertia of the sail and the payload, respectively; c)  $k$  and  $c$ , the spring constant and the viscous coefficient of each degree of freedom of the universal joint. The design objective is to damp out the large initial forced precession cone angle as well as any wobble motion of the system.

From energy consideration, it is clear that in order to damp out the forced precession, a large part of the total energy of the system has to be dissipated. Therefore, to obtain a reasonable damping time it is necessary to use a damper whose moments of inertia are comparable in size with those of the main body ( $\rho \approx 1$ ). This is already

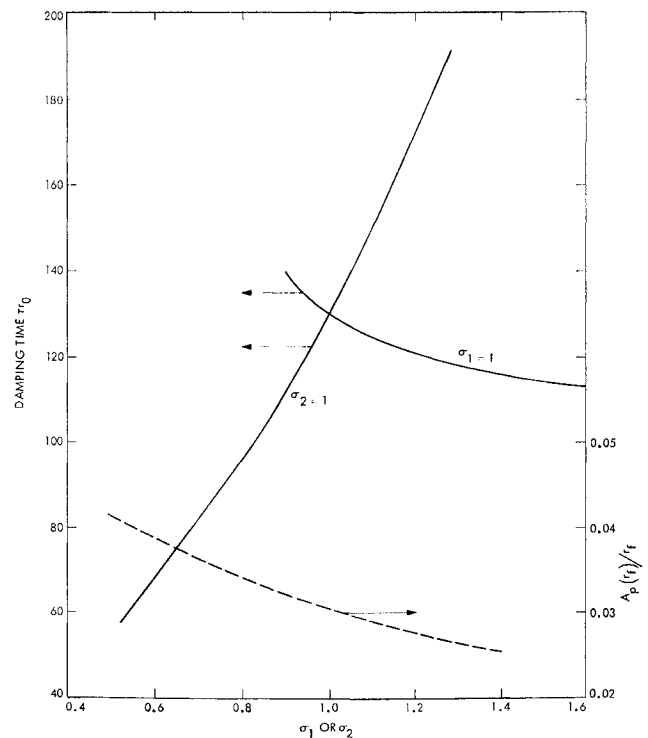


Fig. 2 Damping time and amplitude ratio  $A_p/r$  vs  $\sigma_1$  and  $\sigma_2$ .

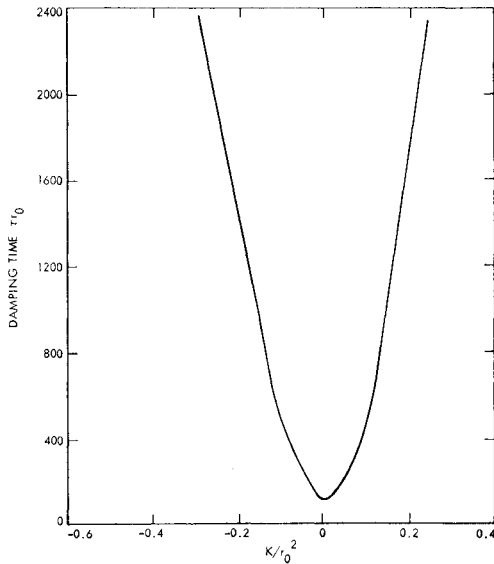


Fig. 3 Damping time vs  $K/r_0^2$ .

achieved by using an existing mass of the system, the solar sail.

To study the effects of  $\sigma_1$  and  $\sigma_2$  on the response of this system, we will examine the steady-state response of Eqs. (21) and (22). Let  $A_p$  and  $A_\alpha$  be the amplitudes of  $p$  and  $\alpha$ , respectively. From the symmetry of the system we expect  $A_q = A_p$  and  $A_\alpha = A_\beta$ . The two quantities of particular interest here are a) the damping time  $\tau$  of the forced precession cone angle, and b)  $A_p/r$ , the ratio between the transverse and the axial angular velocity of the sail, which indicates the tendency for the system to wobble.

Damping time  $\tau$  can be computed by using Eq. (20) or (12) once  $A_\alpha(r)$  is known. In computing  $A_\alpha(r)$ , we have used the relationships  $\sin\theta = 1 - \cos^2\theta = 1 - (r_0 \cos\theta/r)^2$  from Eq. (8) where  $\theta_0$  and  $r_0$  are the initial cone angle and spin rate, respectively.

Figure 2 shows  $\tau r_0$  (to reduce  $\theta$  from  $60^\circ$  to  $5^\circ$ ) as a function of  $\sigma_1$  (with  $\sigma_2 = 1, \rho = 1, K/r_0^2 = 0, D/r_0 = 0.1, (P/A')/r_0^2 = 0.1$ ). It is seen that  $\tau r_0$  increases almost linearly with  $\sigma_1$ . In other words, to minimize  $\tau r_0$ , one would like to use a slender sail with the ratio of its axial to transverse moment of inertia  $< 1$ . (The range of both  $\sigma_1$  and  $\sigma_2$  is from 0 to 2.) Figure 2 also shows  $\tau r_0$  vs  $\sigma_2$  (with  $\sigma_1 = 1$ , the other parameters same as before.) Here,  $\tau r_0$  decreases with increasing  $\sigma_2$ . Therefore, to reduce  $\tau$  it is desirable to have a disc

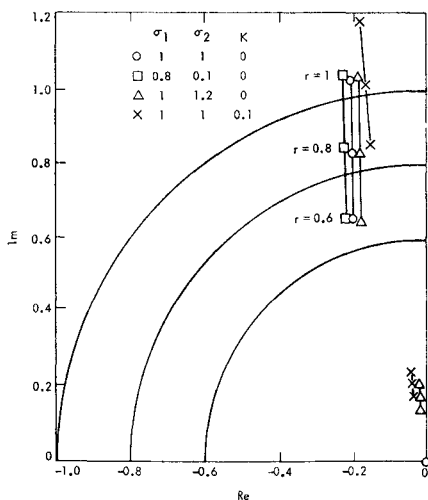


Fig. 4 Root loci as a function of spin rate  $r$ .

shape payload with the ratio of its axial to transverse moment of inertia greater than 1.

Finally, Fig. 2 shows  $A_p(r_f)/r_f$  vs  $\sigma_1$ , where  $r_f$  is the final value of the spin rate (here  $\sigma_2 = 1$ , the other parameters same as before; the dependence on  $\sigma_2$  with  $\sigma_1 = 1$  is exactly the same). It is seen that  $A_p/r$  increases with decreasing  $\sigma_1$ , which indicates the tendency for the system to wobble when  $\sigma_1 < 1$ . This tendency is also seen from a root locus plot (as a function of spin rate) of the system, Fig. 4. For  $\sigma_1 < 1$ , the system has a pair of unstable poles.

Figure 3 shows the dependence of  $\tau r_0$  upon  $K/r_0^2$  ( $\sigma_1 = \sigma_2 = 1$ , other parameters same as before). There is a very sharp minimum at  $K/r_0^2 = 0$ . The explanation is as follows. Since the primary frequency experienced by the damper is the spin rate, to improve the effectiveness of the damper requires keeping the damper's natural frequency as close as possible to  $r$  as the system despins gradually. This is indeed the case when  $K = 0$  as seen from the root locus plot as a function of spin rate in Fig. 4.

To check on the foregoing conclusions, a few attitude trajectories (longitude vs latitude, with the sun as origin) of the two symmetry axes of the system are shown in Figs. 5 and 6, which were obtained by numerically integrating the complete nonlinear equations of motion of the system [Eqs. (A1-A4)]. Figure 5 shows the datum case where  $\sigma_1 = \sigma_2 = 1, K/r_0^2 = 0, D/r_0 = 0.1, (P/A')/r_0^2 = 0.1$ . Physically, the payload lags behind the sail such that a large angle is maintained between their symmetry axes. In this position, the spin motion of the system forces the dampers, which are coincident with each degree of freedom of the universal joint, to move at large amplitude oscillations. This is the main mechanism of forced precession damping. Note that at the terminal time ( $\tau r_0 = 100$ ) there is hardly any wobble of either the sail or the payload.

Figure 6 shows the case when  $\sigma_1$  is reduced to 0.8 (the other parameters being the same). In agreement with the previous conclusion, wobble motion builds up after the forced precession is damped out. This instability inhibits the use of a slender sail ( $\sigma_1 < 1$ ) to improve the damping time.

#### An Analytic Solution

For the special configuration mentioned, where the axial and transverse moment of inertia are equal in both bodies, it has been found that the best value of  $K$  for tuning purposes is zero. For  $K = 0$ , the characteristic equation of the

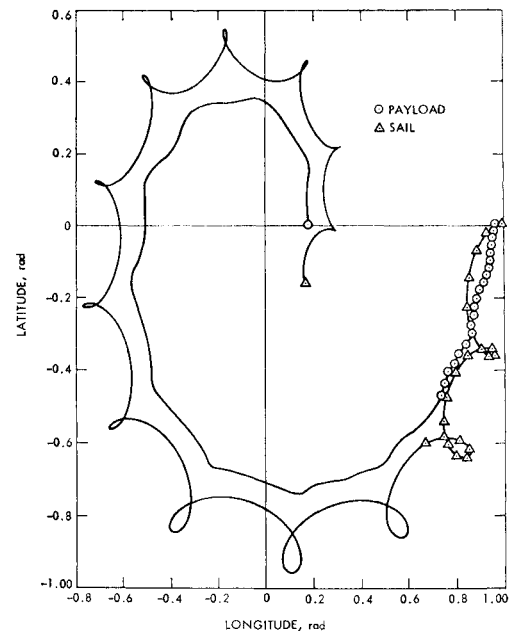


Fig. 5 Attitude trajectories ( $\sigma_1 = \sigma_2 = 1$ ).

system in Eqs. (21) and (22) reduces to

$$s^4[s^2 + 2D(1 + \rho)s + D^2(1 + \rho)^2 + r^2] = 0 \quad (23)$$

Equation (23) has a quadruple root at the origin and one pair of complex roots at

$$s = -D(1 + \rho) \pm jr \quad (24)$$

The frequency response of the damper now becomes

$$A_\alpha = A_\beta = (P/A') \sin\theta/(1 + \rho)Dr \quad (25a)$$

$$\Psi = 90^\circ \quad (25b)$$

Then, the design of this damper reduces to selecting the proper damping coefficient at the joint such that at the initial spin rate  $r_0$  and precession cone angle  $\theta_0$ ,  $A_\alpha$ , and  $A_\beta$  do not exceed the maximum travel of the damper mass  $\alpha_m$ .

$$D \geq (P/A') \sin\theta_0/(1 + \rho)r_0\alpha_m \quad (26)$$

Because of the simple form of  $A_\alpha$  and  $\Psi$  in Eq. (25), it is possible in the following to evaluate analytically the quadratures in Eqs. (12) and (20), both of which give the damping time  $t$  of the precession cone angle.

Let  $\bar{\alpha}$  and  $\bar{\beta}$  be the envelope of  $\alpha$  and  $\beta$ , respectively. The rate of energy dissipation can be expressed as

$$\dot{E} = -\frac{1}{2}I_1D(\dot{\bar{\alpha}}^2 + \dot{\bar{\beta}}^2)$$

Substitution of Eq. (25) into this expression of  $\dot{E}$  gives

$$\dot{E} = -(I_1/D)(P/A')^2(1/1 + \rho)^2 \sin^2\theta \quad (27)$$

Since the total energy of the system  $E$  consists mainly of the spin kinetic energy, we have

$$E = \frac{1}{2}(C + I_3)r^2 \quad (28)$$

With the above expressions for  $E$  and  $\dot{E}$ , Eq. (12) reduces to

$$t(\theta) = \frac{1}{\omega_L^4} \frac{(1 + \rho)^3}{\rho} D \int_{\cos\theta_0}^{\cos\theta_f} \frac{r^2 d \cos\theta}{\cos\theta \sin^2\theta} \quad (29)$$

where  $\omega_L^2 \equiv P/A'$ . By the use of the angular momentum relation, Eq. (8), the integral above is evaluated.

$$t(\theta)/T = (1/\cos^2\theta_0 - 1/\cos^2\theta_f) + 2 \ln(\tan\theta_0/\tan\theta_f) \quad (30)$$

where

$$T = \frac{1}{2}(r_0/\omega_L^2)^2[(1 + \rho)^3/\rho]D \cos^2\theta_0$$

Similarly, the quadrature in Eq. (20) can be carried out by substituting Eq. (25) for  $A_\alpha$ :

$$t(\theta_f, \theta_0) = \frac{T}{g} \left[ \frac{r_0^2 - r_f^2}{r_z^2} + \ln \frac{r_0^2 - r_z^2}{r_f^2 - r_z^2} \right] \quad (31)$$

where  $r_z \equiv r_0 \cos\theta_0$ . By a change of variable, it can be shown that Eq. (31) is exactly equivalent to Eq. (30) when  $g = 1$ .

In order to prevent the damper from hitting its stop, the proper value of the viscous coefficient at the joint has a lower limit as in Eq. (26). From Eqs. (26) and (30), the lower bound on the damping time is obtained.

$$t(\theta_f, \theta_0) \geq T_D f(\theta_f, \theta_0) \quad (32)$$

where

$$T_D \equiv \frac{1}{2}(r_0/\omega_L^2)(1 + \rho)^2/\rho(1/\alpha_m) \quad (33)$$

$$f(\theta_f, \theta_0) = \sin\theta_0 \cos^2\theta_0 \left[ \frac{1}{\cos^2\theta_0} - \frac{1}{\cos^2\theta_f} + 2 \ln \left( \frac{\tan\theta_0}{\tan\theta_f} \right) \right] \quad (34)$$

Equations (26) and (32) are summarized in Table 1. Notice that  $T_D$  has the dimension of time that is a function of the system parameters ( $r_0/\omega_L^2$ ),  $\rho$ , and  $\alpha_m$ . It represents the time scale of the precession damping problem. From Eq. (33) it is seen that  $T_D$  has a minimum at  $\rho = 1$ . This important result agrees with the intuitive reasoning that maximum damping is achieved when the two parts of the system are of the same size (moment of inertia).

Figure 7 shows the function  $f(\theta_f, \theta_0)$  when  $\theta_f$  equals 0.05 rad. It displays the dependence of  $t$  on the initial cone angle  $\theta_0$ . It is interesting to find that  $f$  has a maximum at  $\theta_0 \cong 0.8$  rad rather than being a monotonically increasing function of  $\theta_0$ . This implies that for two systems with the same initial spin rate, the one with the larger initial cone angle may erect itself faster than the one with the smaller initial cone angle.

### Example

This example illustrates the application of the newly developed theory on the damping of forced precession motion

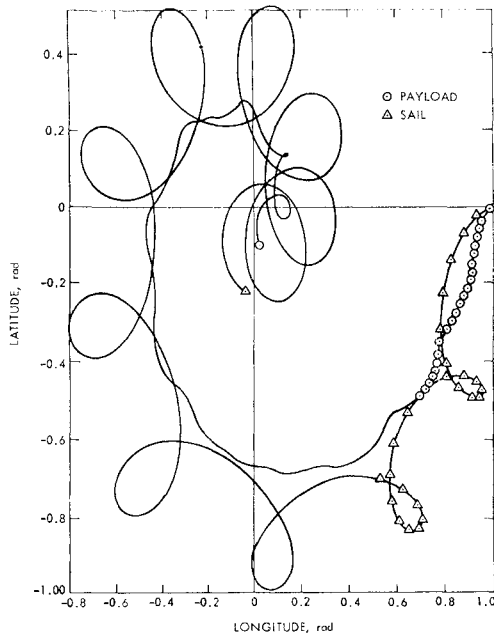


Fig. 6 Attitude trajectories ( $\sigma_1 = 0.8$ ,  $\sigma_2 = 1$ ).

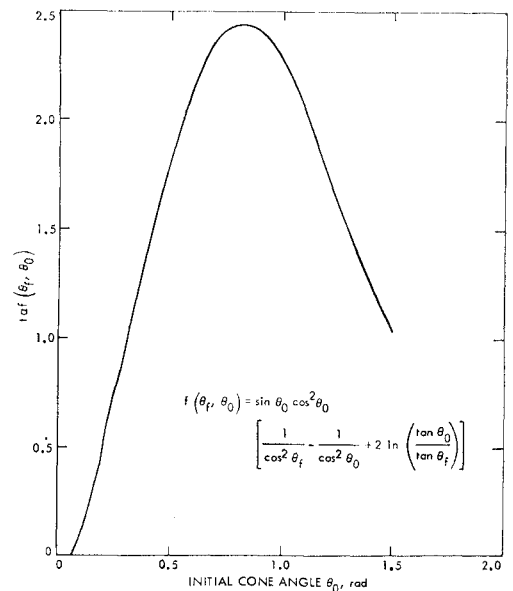


Fig. 7 The dependence of damping time  $t$  on the initial cone angle.

to the design of a small sun-pointing interplanetary probe weighted about 30 lb. The vehicle consists of a short cylindrical shape payload and a smooth total reflecting conical solar sail connected by a lossy universal joint (see Table 1). The spacecraft, at injection, is spinning about its symmetry axis oriented  $60^\circ$  away from the payload-sun line. Immediately after its separation from the rocket motor, the spin rate of the vehicle is reduced from the initial value of 30 rpm to 1 rpm by a "yo-yo" despin device. The sail is then deployed. The attitude stabilization problem consists of two phases: a) the initial erection of the symmetry axis toward the sun and b) the keeping of the symmetry axis pointing toward the sun as the vehicle travels on an elliptical path around the sun. We will consider here only the design problem associated with the first phase. The objective is to minimize the erecting time required.

Since the surface area of the payload is much smaller than the sail, it is assumed that solar-pressure torque acts only on the sail. It is further assumed that the external torque varies sinusoidally with the angle between the sun vector and the symmetry axis of the sail. These idealizations of the solar-pressure torque is close to that of a conical sail with total reflecting surface.<sup>9</sup> Detail design and calculation of the force and torque curves of a variety of solar sails can be found in Ref. 9.

The assumed values for the physical parameters of the system are summarized in Table 2.

From Table 2, the following quantities are obtained:

$$\omega_L^2 = P / \left( A + \frac{m_s m_p a^2}{m_s + m_p} \right) = 0.0001 (\text{rad/sec})^2$$

$$a = (\sin \theta_0) / \alpha_m = 2.1$$

$$\rho = I_1 / \left( A + \frac{m_s m_p a^2}{m_s + m_p} \right) = 1.39$$

It remains to determine the spring constant  $k$  and viscous coefficient  $c$  of the joint. From Table 1, we have  $c = r_0 a - (\omega_L / r_0)^2 I_1 / (1 + \rho) = 1.76 \times 10^4 \text{ dyn-cm/(rad/sec)}$ ,  $k = 0$ , and  $T_D = \frac{1}{2} (r_0 / \omega_L^2) (1 + \rho)^2 / \rho \alpha_m = 5100 \text{ sec}$ . Now the system is completely specified. The motion of the system has been obtained by numerically integrating the exact nonlinear equations of motion of the system [Eqs. (A1-A4)]. The following initial conditions were used in the integration:  $p = q = 0$ ,  $r = 0.1 \text{ rad/sec}$ ,  $W_1 = W_2 = 0$ ,  $W_3 = 0.1 \text{ rad/sec}$ ,  $\alpha = \beta = \theta_1 = \theta_3 = 0$ , and  $\theta_2 = 1 \text{ rad}$ .

Time histories of  $\alpha$ ,  $r$ , and  $\theta$  are shown in Fig. 8. The accuracy of the numerical integration is checked by computing a constant of motion of the system. At the end of the integration ( $t = 20,000 \text{ sec} = 5.55 \text{ hr}$ ), the deviation of

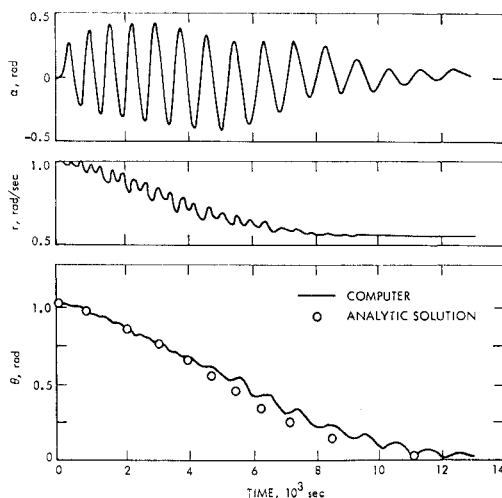


Fig. 8 Time histories of  $\theta$ ,  $\alpha$ ,  $r$  without initial wobble.

Table 2 Physical parameters

Payload
$m_s$ , mass = 10,000 g
$I_3$ , axial moment of inertia = $2.5 \times 10^6 \text{ g-cm}^2$
$I_1, I_2$ , transverse moment of inertia = $2.5 \times 10^6 \text{ g-cm}^2$
Solar sail
$m_p$ , mass = 1000 g
$C$ , axial moment of inertia = $1.8 \times 10^6 \text{ g-cm}^2$
$A, B$ , transverse moment of inertia = $1.28 \times 10^6 \text{ g-cm}^2$
$d$ , distance of the joint from the c.m. of the sail = 25 cm
Initial spin rate and cone angle
$r_0 = 0.1 \text{ rad/sec}$ , $\theta_0 = 1 \text{ rad}$
Solar-pressure-torque constant (about c.m. of the sail):
$P = 180 \text{ dyn-cm/rad}$
Maximum travel of the joint: $\alpha_m = 0.4 \text{ rad}$

that constant from its nominal value is less than 0.2%. The computer time used is less than 1 min of IBM 360 computer. It is seen in Fig. 8 that  $\theta$  is reduced from 1 to 0.02 rad in less than 3.7 hr, which is quite acceptable for this type of spacecraft. The final spin rate is 0.051 rad/sec ( $\sim 0.5 r_0$ ).

For comparison purpose, the envelope of the  $\theta$  motion as predicted analytically by using Table 1 is shown in the same figure where close agreement is observed. It is therefore concluded that the analytic results from the simplified theory developed can be used with confidence in the preliminary design of this class of forced precession damping systems.

Figure 9 shows the time history of  $\theta$  when the system has small initial wobbling motion [ $p(0) = W_1(0) = 0.02 \text{ rad/sec}$ ]. It is interesting to note that the final  $\theta$  angle is nonzero. This points to the fact that because  $I_1 = I_2 = I_3$  and there is no spring constraint at the joint, the orientation of the payload with respect to the sail is neutrally stable. To circumvent this shortcoming, it was decided to make the axial moment of inertia of the payload greater than its transverse moment of inertia ( $I_3/I_1 = 1.17$ ). The resulting time history of  $\theta$  is shown also in Fig. 9 for comparison. It is observed that the added stability is obtained, at the cost of a slightly longer damping time compared with the original design.

## Discussion

The slow rotation of the solar radius vector corresponding to the orbital angular velocity of the satellite prevents the spin axis from ever being completely aligned with the radius vector. For a circular orbit, the constant orbital rate will cause the spin axis to precess at some small equilibrium cone angle. An investigation into the stability of this small precession motion as well as the long-term behavior of the spin rate is nearly completed and will be reported in a subsequent paper. For an elliptic orbit, both the orbital rate

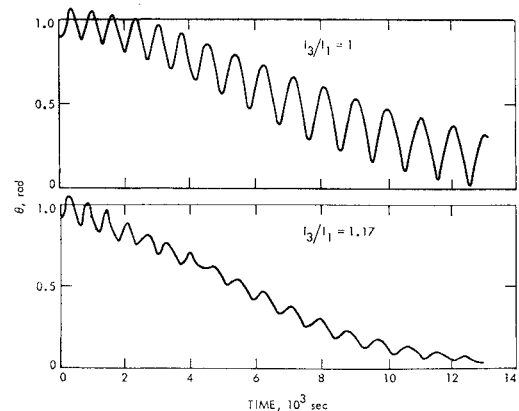


Fig. 9 Time histories of  $\theta$  with initial wobble.

and the solar-torque constant  $P$  vary periodically at the orbital period. The stability of this parametric excited system remains to be resolved.

In conclusion, the simplified theory developed in this paper was found to be adequate for predicting the damping time of the transient oscillations of the system.

Although Table 1 applies only to the special configuration where  $A' = B' = C$  and  $I_1 = I_2 = I_3$ , it is also useful as a guideline in the preliminary design of forced-precession dampers that are only slightly different from this near-optimum configuration.

The special appeal of the present attitude stabilization scheme is its simplicity and ease of mechanization. The fact that no spring torque at the joint is required for tuning eliminates the problem of material fatigue and critical alignment of a spring element.

### Appendix: Equations of Motion

$$\dot{p} = F_1, \dot{q} = F_2 + (M_z S_\alpha)/B' \quad (A1a)$$

$$\dot{r} = F_3 - (M_z C_\alpha)/C \quad (A1b)$$

$$\dot{W}_1 = F_4 - (M_z S_\beta)/I_1, \dot{W}_2 = F_5 \quad (A2a)$$

$$\dot{W}_3 = F_6 + (M_z C_\beta)/I_3 \quad (A2b)$$

$$\dot{\alpha} = F_7, \dot{\beta} = F_8 \quad (A3)$$

where

$$F_1 = [(B' - C)qr + T_{pz} - M_\alpha]/A' \quad (A4a)$$

$$F_2 = [(C - A')pr + T_{py} - M_\beta C_\alpha]/B' \quad (A4b)$$

$$F_3 = [(A - B)pq + T_{pz} - M_\beta S_\alpha]/C \quad (A4c)$$

$$F_4 = [(I_2 - I_3)W_2W_3 + M_\alpha C_\beta]/I_1 \quad (A4d)$$

$$F_5 = [(I_3 - I_1)W_1W_3 + M_\beta]/I_2 \quad (A4e)$$

$$F_6 = [(I_1 - I_2)W_1W_2 + M_\alpha S_\beta]/I_3 \quad (A4f)$$

$$F_7 = W_1C_\beta + W_3S_\beta - p \quad (A4g)$$

$$F_8 = W_2 - qC_\alpha - rS_\alpha \quad (A4h)$$

$$F_z = -(qC_\alpha + rS_\alpha)F_7 + (W_1C_\beta + W_3S_\beta)F_8 \quad (A4i)$$

$$M_\alpha = -k\alpha - c\dot{\alpha}, M_\beta = -k\beta - c\dot{\beta} \quad (A5a)$$

$$M_z = (-S_\alpha F_2 + C_\alpha F_3 + S_\beta F_4 - C_\beta F_6 - F_z)/\Delta \quad (A5b)$$

$$\Delta = \frac{S_\alpha^2}{B'} + \frac{C_\alpha^2}{C} + \frac{S_\beta^2}{I_1} + \frac{C_\beta^2}{I_3} \quad (A5c)$$

$$T_{pz} = -P \sin\theta_2 \sin\theta_3 \quad (A6a)$$

$$T_{py} = -P \sin\theta_2 \cos\theta_3, T_{pz} = 0 \quad (A6b)$$

### References

- <sup>1</sup> Donatoni, A., "Passive Attitude Stabilization of an Interplanetary Probe," *Attitude Changes and Stabilization of Satellite*, Colloque International, Paris, Oct. 1968, pp. 151-175.
- <sup>2</sup> Sohn, R. L., "Attitude Stabilization by Means of Solar Radiation Pressure," *ARS Journal*, Vol. 29, May 1959, pp. 371-373.
- <sup>3</sup> Frye, W. E. and Sterns, E. V. B., "Stabilization and Attitude Control of Satellite Vehicles," *ARS Journal*, Vol. 29, Dec. 1959, pp. 927-931.
- <sup>4</sup> Hibbard, R. R., "Attitude Stabilization Using Focused Radiation Pressure," *ARS Journal*, Vol. 31, June 1961, pp. 844-845.
- <sup>5</sup> Acord, J. D. and Nicklas, J. C., "Theoretical and Practical Aspects of Solar Pressure Attitude Control for Interplanetary Spacecraft," *Guidance and Control II*, edited by R. C. Langford and C. J. Mundo, Academic Press, New York, 1963, pp. 73-101.
- <sup>6</sup> Ule, L. A., "Orientation of Spinning Satellite by Radiation Pressure," *AIAA Journal*, Vol. 1, No. 7, July 1963, pp. 1575-1578.
- <sup>7</sup> Peterson, C. A., "Use of Thermal Radiation Effects in Spacecraft Attitude Control," CSR R-66-3, 1966, Center for Space Research, MIT, Cambridge, Mass.
- <sup>8</sup> Colombo, G., "Passive Stabilization of a Sunblazer Probe by Means of Radiation Pressure Torque," CSR TR-66-5, 1966, Center for Space Research, MIT, Cambridge, Mass.
- <sup>9</sup> Falcovitz, J., "Attitude Control of a Spinning Sun-Orbiting Spacecraft by Means of a Grated Solar Sail," CSR TR-66-17, 1966, Center for Space Research, MIT, Cambridge, Mass.